Micro-excavation and direct chemical analysis of individual fluid inclusion by cryo-FIB-SEM-EDS: Application to the UHP talc-garnet-chloritoid schist from the Makbal Metamorphic Complex, Kyrgyz Tian-Shan

KENTA YOSHIDA,[1]* RUSTAM OROZBAEV,[2] TAKAO HIRAJIMA,[3] AKIRA MIYAKE,[3] AKIRA TSUCHIYAMA,[3]
APAS BAKIROV,[2] AKIRA TAKASU[4] and KADYRBEK SAKIEV[2]

[1]Research and Development Center for Ocean Drilling Science, Japan Agency for Marine-earth Science and Technology,
Yokosuka 237-0061, Japan
[2]Institute of Geology, Kyrgyz National Academy of Sciences, 30 Erkindik Avenue, 720040 Bishkek, Kyrgyzstan
[3]Department of Geology and Mineralogy, Kyoto University, Kyoto 606-8502, Japan
[4]Department of Geoscience, Shimane University, Matsue 693-8501, Japan

Direct chemical analysis of a single fluid inclusion was conducted by micro-excavation at cryo-temperatures. A scanning electron microscope (SEM) equipped with a focused ion beam (FIB), an energy dispersive X-ray spectrometer (EDS), and a cold stage, were used to analyze the chemical composition of the sample fluid inclusion, which was trapped in the ultrahigh-pressure (UHP) talc-garnet-chloritoid schist obtained from the Makbal metamorphic complex, Kyrgyz. Conventional techniques such as microthermometry and cryo-temperature and room-temperature Raman spectroscopy enabled the detection of NaCl and CaCl$_2$ as solute species in the fluid inclusions, as well as high salinity of 20.5 mass% CaCl$_2$ and 1.7 mass% NaCl with the assumption of a NaCl-CaCl$_2$-H$_2$O ternary system. However, additional chemical analysis using the present cryo-FIB-SEM-EDS system further revealed the presence of K as a solute element, which is hardly identified by conventional techniques.

Petrographic examination of the fluid inclusions indicated that they had been trapped during the exhumation stage of the UHP talc-garnet-chloritoid schist, possibly originating from the decompression breakdown of lawsonite. The data acquired from the present study challenges previous reports of the existence of simple chemical system of aqueous fluids in high-pressure and UHP metamorphic terrane in eastern Asia. This is imperative because misidentification of solute species introduces errors into salinity estimation, resulting in inaccuracy propagation in quantitative analytical processes such as LA-ICP-MS. A detailed fluid inclusion petrography would thus require accurate quantitative analysis involving FIB-based sample-preparation and SEM-EDS analysis.

Keywords: fluid inclusion, focused ion beam, Raman spectroscopy, ultrahigh-pressure metamorphism, Kyrgyz Tian-Shan

INTRODUCTION

Aqueous fluids in convergent plate boundaries play important roles in geochemical and geophysical processes, such as trigger of arc magmatism and seismicity, and element transfer (e.g., Scambelluri and Philippot, 2001). Under cold subduction settings, lawsonite is one of the most important water-carriers and remains stable up to ultrahigh pressure (UHP) conditions (e.g., Tsujimori *et al.*, 2006). In the early stage of subduction, dehydrated fluids from low-grade minerals such as chlorite are consumed in the formation of lawsonite, resulting in the suppressed release of bulk H$_2$O (Kuwatani *et al.*, 2011; Sato *et al.*, 2016).

The varying composition of metamorphic fluids affects their hydration/dehydration reactions. Generally, high-salinity fluids exhibit low H$_2$O activities, and therefore, shift dehydration reactions to lower-temperature conditions and significantly change the solubility of minerals (e.g., Newton and Manning, 2010). Previous studies mainly focused on NaCl-rich aqueous fluids due to their ubiquitous occurrence in metamorphic rocks, although numerous works have also reported the existence of other salts such as CaCl$_2$ and KCl, especially in continental collision zones (e.g., Gao and Klemd, 2001; Okudaira *et al.*, 2017).

Phase diagrams and microthermometry are commonly employed in the determination of the chemical compositions of fluid inclusions (e.g., Bodnar, 1993). However, the application of microthermometry to small inclusions measuring as little as a few microns is hampered by the difficulty of optical observation of the phase transition

---
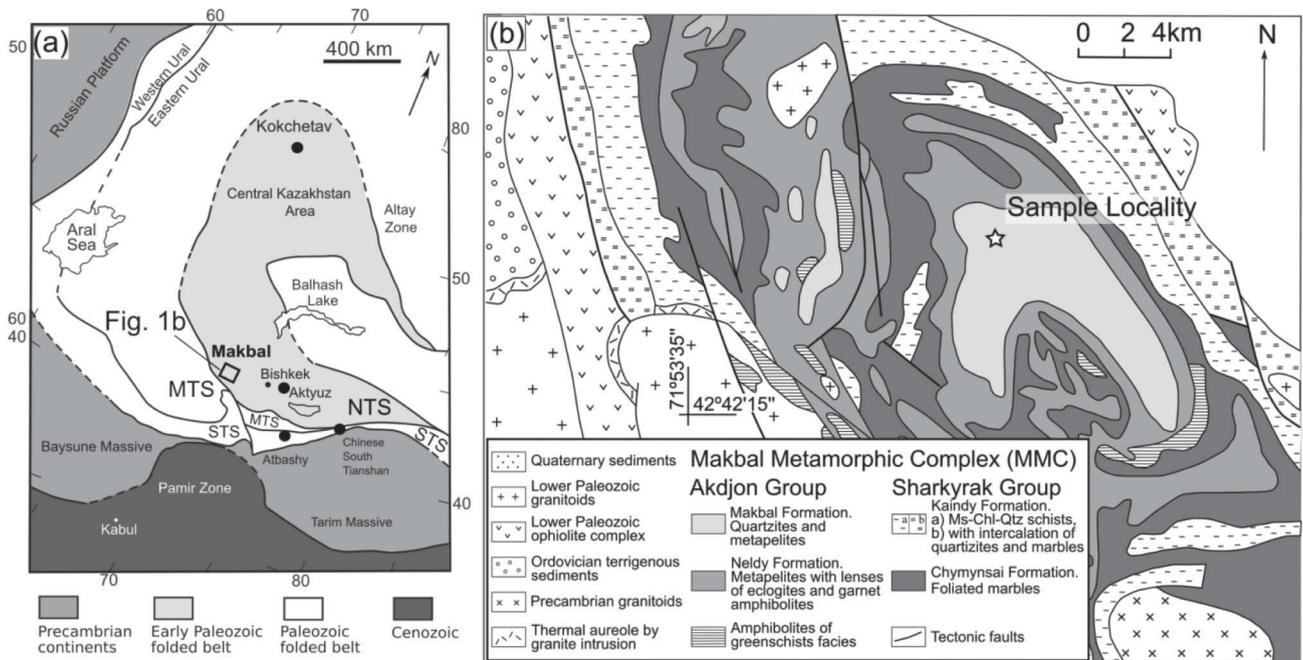
*Corresponding author (e-mail: yoshida_ken@jamstec.go.jp)

Fig. 1. (a) Geological overview of the tectonic units of central Asia after Bakirov et al. (1998). NTS - Northern Tien-Shan; MTS - Middle Tien-Shan; STS - Southern Tien-Shan. (b) Geologic map of the Makbal UHP metamorphic complex composed of the Akdjon and Sharkyrak Groups. Sample locality of the studied sample is also shown.

(e.g., Raimburg *et al*., 2014). Furthermore, if there are more than four types of electrolytes, estimation of chemical compositions of the inclusion based on the phase diagram would be almost impossible (e.g., Spencer *et al*., 1990). Researchers of fluid inclusions have therefore developed several techniques for directly analyzing the chemical composition of individual inclusions over the past quarter century. For example, laser ablation inductively coupled plasma mass spectrometry (LA-ICP-MS), in which a laser beam is used as a boring and vaporizing tool, has been developed for application to inclusions of diameter 15–20 μm (e.g., Heinrich *et al*., 2003). Another method that employs a scanning electron microprobe (SEM) equipped with an energy dispersive X-ray spectrometer (EDS) is used for frozen fluid inclusions at cryo-temperatures (e.g., Ayora and Fontarnau, 1990). This method enables direct quantitative measurement based on comparison of the X-ray intensities for the sample and standard ice. The mineral chip sample containing the frozen fluid inclusions is broken in an evacuated chamber using a manipulator. However, samples prepared by this procedure should ideally contain many inclusions because of the uncertainty of the mechanical breaking. The application of this method has thus been mainly limited to halite-hosted fluid inclusions.

Recent developments and the proliferation of the focused ion beam (FIB) system have enabled the sample processing of an area of interest with very good submicron precision (Reyntjens and Puers, 2001; Wirth, 2004), which can be combined with other high-resolution analysis technique such as SEM, TEM, and micro-X-ray tomography (e.g., Liu *et al*., 2016; Yoshida *et al*., 2016). FIB-based micro-excavation of buried fluid inclusions has been employed for the SEM-EDS analysis of daughter minerals and precipitated salts such as Fe-K(-Mn) chlorides (Assadzadeh *et al*., 2016). However, this novel tool can be combined with a cold stage for application to the direct analysis of liquid materials (i.e., using cryo-FIB; e.g., Desbois *et al*., 2008, 2012), resulting in high-resolution observation of the wet boundaries of minerals. A combination of cryo-FIB-SEM-EDS would significantly enhance the possibility of analyzing the chemical compositions of liquid materials sporadically enclosed in the solid phase, such as fluid inclusions in metamorphic rocks, the sizes and numbers of which commonly limit the application of existing methods.

In the present study, we performed conventional fluid inclusion petrography on Tlc-Grt-Cld schist collected from the Makbal metamorphic complex in Kyrgyz. In addition to textual observation under an optical microscope, Raman analysis at room temperature, and microthermometry, we performed low-temperature Raman (cryo-Raman) analysis of the sample. Finally we attempted cryo-FIB-SEM-EDS analysis of the inclusion to

determine the solute species, although there were challenges to using the same for a quantitative analysis. The determined chemical composition was complex and could not have been established by conventional microthermometry and the cryo-Raman technique. Based on our findings, we propose an importance of a sequential investigation for a single fluid inclusion with respect to the petrographic description. The mineral abbreviations used in this paper follow Whitney and Evans (2010).

GEOLOGICAL BACKGROUND AND INVESTIGATED SAMPLE

The Makbal metamorphic complex is located in the western part of Northern Kyrgyz Tian-Shan (Fig. 1) and consists of two main units, namely, upper Sharkyrak Group characterized by greenschist facies metamorphism, and the lower Akdjon Group that exhibits higher-grade metamorphism (HP-UHP conditions) (Bakirov, 1978; Bakirov *et al.*, 1998; Tagiri *et al.*, 2010). The Akdjon Group is subdivided into the Neldy and Makbal Formations. The Neldy Formation is mainly composed of mica-quartz (±garnet) schists with mafic lenses, some of which (eclogites) show peak P-T metamorphic conditions of 550–610°C and 2.2–2.5 GPa (Togonbaeva *et al.*, 2010). The Makbal Formation consists mainly of quartzites, garnet-mica schists, and marbles (e.g., Bakirov, 1978). Talc-garnet-chloritoid schists are found in the quartzites as layers measuring hundreds of meters to a few kilometers long. UHP metamorphism has been confirmed by the finding of coesite inclusions within garnet from both Tlc-Grt-Cld schists and surrounding quartzites (Tagiri *et al.*, 2010; Orozbaev *et al.*, 2015). The peak P-T conditions of Tlc-Grt-Cld schists have been variously estimated by different methods to be 530–580°C and 2.8–3.3 GPa by petrogenetic grid (Orozbaev *et al.*, 2015) and approximately 580°C and 2.85 GPa by pseudosection modeling (Meyer *et al.*, 2014). Paleozoic metamorphic ages of the Tlc-Grt-Cld schists are reported by different methods; U-Pb SHRIMP age of 502 ± 10 Ma for metamorphic zircon rims (Konopelko *et al.*, 2012), phengite K-Ar age of 509 ± 13 Ma (Tagiri *et al.*, 2010), and Th-Pb CHIME monazite ages of 481 ± 26 Ma and 480 ± 56 Ma (Togonbaeva *et al.*, 2009).

The studied fluid inclusions investigated in the present study existed in a Tlc-Grt-Cld schist collected from the Makbal Formation. The hand-specimen was collected from the outcrop which is investigated in detail by Orozbaev *et al.* (2015). Orozbaev *et al.* (2015) reported that the large garnet porphyroblast and quartz pressure shadows were embedded in the matrix mainly composed of talc and chloritoid. The petrographical description of the studied sample (KG1223) exhibited similar mineral textures and assemblages described by Orozbaev *et al.*

(2015). In this previous study, three stages of mineral assemblages were distinguished, namely, the prograde stage: Grt + Tlc + Ctd + Qz + Chl + Lws + Ap + Rt ± Tur; the peak UHP stage: Grt + Tlc + Ctd + Gln + Coe + Ph + Ap + Rt ± Lws ± Tur ± Ky; and the retrograde stage: Qz + Pg + Mrg + Bt + Chl + Cz + Ky + Ap + Ilm. In the garnet porphyroblast, they reported polyphase mineral aggregates mainly composed of clinozoisite, kyanite, and quartz, the combined bulk composition of which resembles that of lawsonite. Based on a petrogenetic grid, Orozbaev *et al.* (2015) concluded that breakdown of lawsonite had occurred during a nearly-isothermal-decompression of the rock (510–580°C and 1.6–2 GPa). In the following sections, we present a detailed description of the fluid inclusions in quartz pressure shadows newly described in the present study.

ANALYTICAL METHODS

The fundamental fluid inclusion petrography was performed by using optical microscope, a laser Raman spectrophotometer (JASCO, NRS-3100), and a heating and cooling stage (LINKAM, LK-600) at the Department of Geology and Mineralogy, Kyoto University. The Raman spectroscopic analysis was conducted using a 532-nm line of diode-pumped solid-state laser (Cobolt, Samba) at 3–15 mW on the sample surface. Calibration of the wave number was performed using a 520.7-cm^{-1} Si-wafer band and a neon spectrum. To determine the salinity and solute species of the aqueous phase of the fluid inclusions, microthermometric measurements were performed following the procedure of Yoshida *et al.* (2015). Raman spectroscopy under low-temperature conditions (–190°C) was also performed using a combination of the above instruments to obtain the spectra of the ice and chloride hydrates.

In addition, the solute composition of the aqueous fluid was investigated by energy-dispersive X-ray spectrometry (EDS) using a focused ion beam (FIB) system (Helios NanoLab G3 CX, FEI) at the Department of Geology and Mineralogy, Kyoto University. A gallium ion source installed at an angle of 52° was used to bore and polish the sample. The cryo-preparation of the sample was performed using a cold stage (C1001, Gatan), and the X-ray spectra were obtained by an EDS system (Octane Elite 25, EDAX). The quartz chip containing the fluid inclusions was carbon coated and placed on the cold stage in the FIB evacuated chamber. The cold stage was then cooled and maintained at approximately –130°C by the circulation of cold nitrogen gas. After determining the position of the target fluid inclusion, micro-excavation was performed using the gallium ion beam at 30 kV and 2.5–9.5 nA until the cross section of the frozen inclusion was exposed. EDS analysis was then performed on the
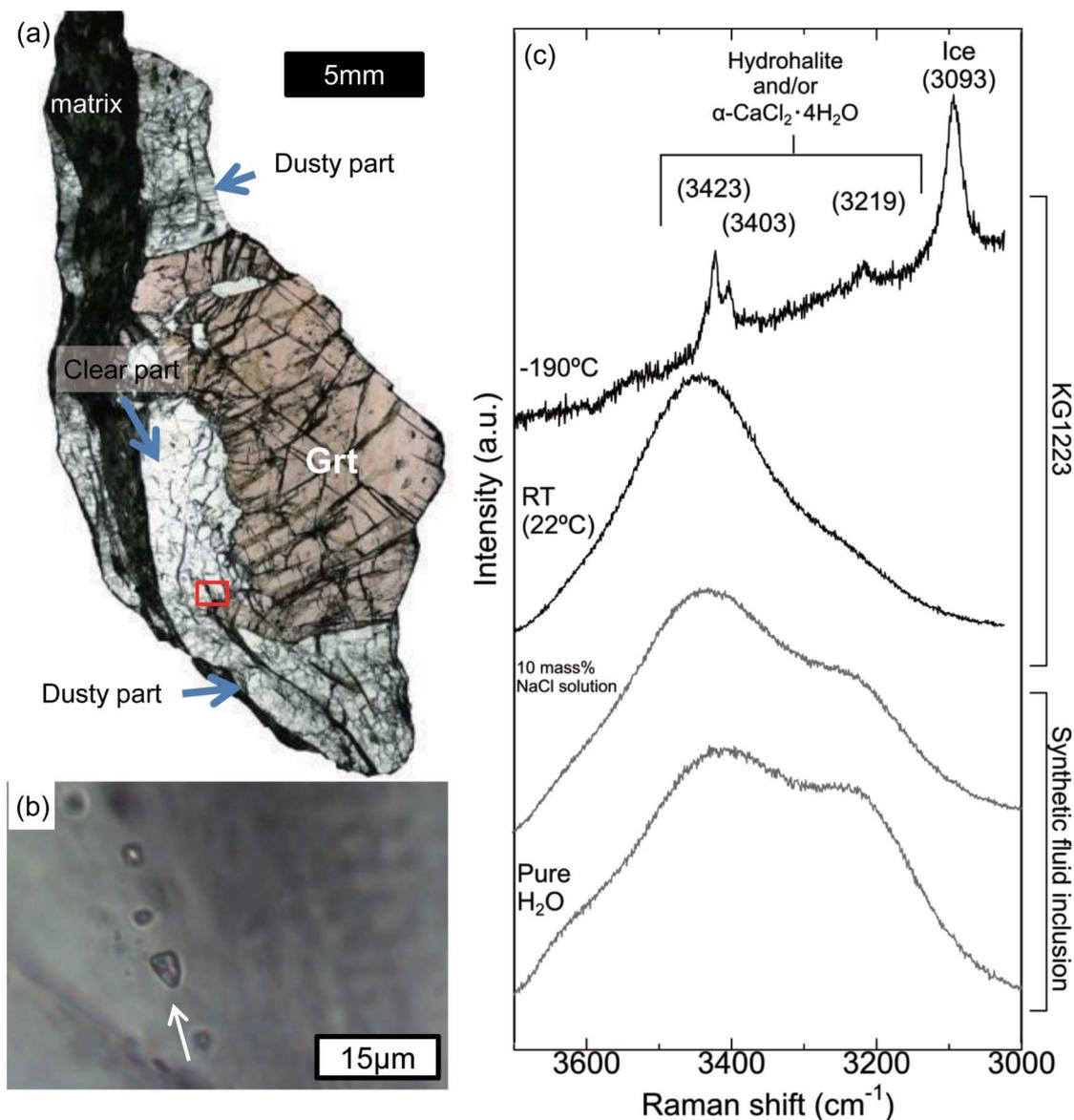
Fig. 2. (a) Scan of the garnet porphyroblast and corresponding quartz pressure shadows. Red rectangle shows the location of the studied fluid inclusion trail. Scale bar is 5 mm. Matrix is mainly composed of chloritoid, talc, and Na-amphibole. (b) Studied fluid inclusions arranged at a certain plane observed under transmitted light. The white arrow indicates the inclusion investigated by cryo-FIB-SEM-EDS. (c) Typical Raman spectra of the studied fluid inclusion measured at room temperature and $-190\,°C$. Liquid H_2O peaks measured at room temperature show a single strong peak with weak shoulder indicating high salinity. For a comparison, Raman spectra of synthetic fluid inclusions (pure water and 10 mass% NaCl aqueous solution) are also shown.

exposed cross section of the inclusion at an acceleration voltage of 15 kV and beam current of 0.34 nA. The X-ray spectra of the exposed cross section, tilted at 38° from the horizontal plane, were obtained, with the tilt causing the EDS detector to be partly blindfolded by the excavated wall of the host phase (quartz). This geometric arrangement precluded quantitative analysis of the peak intensity by ordinary quantification calculation. The EDS result was used only for checking the existence of the detected elements.

RESULTS OF THE FLUID INCLUSION PETROGRAPHY AND CHEMISTRY

Large pressure shadows were found to have developed along the garnet porphyroblasts of up to 10–20 mm in
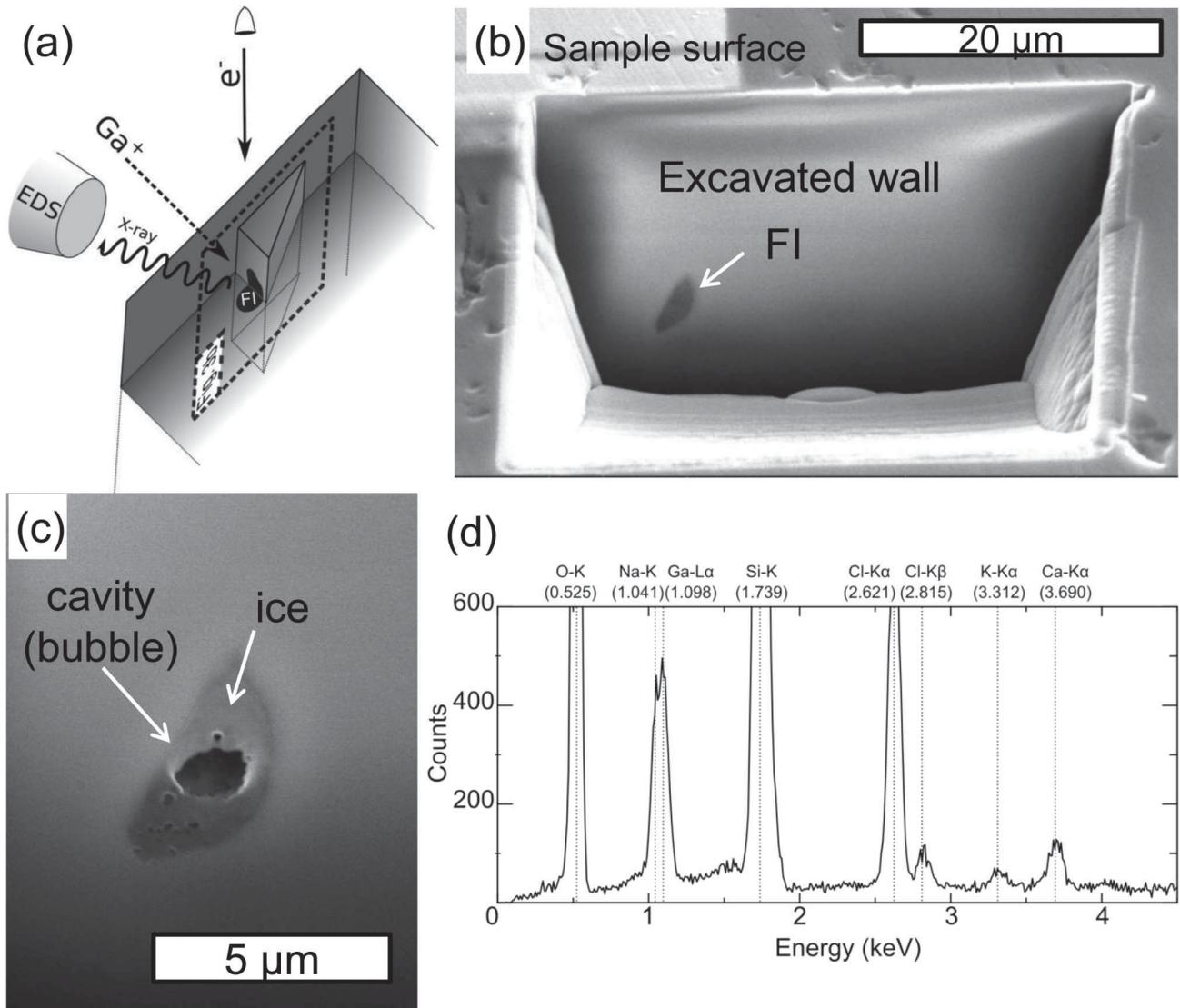
Fig. 3. (a) Schematic image of geometric relationship between the sample surface, fluid inclusion (FI), and (b). (b) SEM image of the frozen fluid inclusion exposed on the excavated wall. (c) Another cross-section of the same fluid inclusion. A large cavity that has been originally a bubble is observed. (d) A representative EDS spectrum of the frozen fluid. Na, K, Ca, and Cl are observed as the solute elements. Ga peak from the plugged gallium ion and Si peak from the host quartz are also observed.

diameter (Fig. 2a). The pressure shadows could be divided into two domains, namely, a dusty part developed in the direction of the main foliation, and a clear part developed along the roof of the host garnet. In the dusty part, several trails of tiny fluid inclusions were observed in the direction perpendicular to the main foliation, having possibly originated from a later stage deformation taken place after the development of the pressure shadows. The clear part appeared to occur as the embayment of the garnet. It contained high-salinity fluid inclusions arranged on the intracrystalline planes, which did not cut across the grain boundaries (Fig. 2b). These observations suggest that the fluid inclusions were trapped simultane-ously with the formation of the pressure shadows. The inclusions were weakly faceted, but did not have clear negative crystal shapes, with their maximum size being <10 μm along the longer axis.

The Raman spectra of a sample fluid inclusion obtained at room temperature showed liquid H_2O peaks showing a single strong peak at around 3450 cm^{-1} with a weak shoulder at lower wavenumber, indicating high salinity compared to the pure water and 10 mass% NaCl aqueous solution (Fig. 2c). No gas species were detected. Conversely, the Raman spectra obtained under low temperature (–190°C) yielded an intense ice peak at 3093 cm^{-1}. Other peaks were observed within 3200–3500

cm^{-1}, attributed to hydrohalite (3403 and 3423 cm^{-1}) and α-CaCl$_2$·4H$_2$O (3219 cm^{-1}) (e.g., Samson and Walker, 2000; Baumgartner and Bakker, 2010).

The microthermometry results showed that, at a temperature lower than –50°C, the liquid phase of the fluid inclusion was completely transformed into solid phase. During heating, the solid phase began to melt at about –48°C, suggesting the existence of dissolved CaCl$_2$. One kind of the solid phases disappeared at –45.5°C, which corresponds to the melting point of hydrohalite. Finally, the ice disappeared at –23.1°C, suggesting that all the observed melting events were explained by the phase relationship of the CaCl$_2$-NaCl-H$_2$O system. The salinity was roughly calculated using AqSo in the FLUIDS software package (Bakker, 2003), assuming CaCl$_2$-NaCl-H$_2$O ternary system. The results indicated 20.5 mass% CaCl$_2$ and 1.7 mass% NaCl as the dissolved salts. However, the chemical system used for the calculation was incorrect as described below.

The chemical composition of the dissolved salts was further investigated by cryo-FIB-SEM-EDS. The frozen fluid inclusion was clearly exposed on the excavated surface of the host quartz (Figs. 3a and b). The cross section of the fluid inclusion appeared weakly faceted, although no clear negative crystal shape of the quartz was observed. After exposure of the edge of the fluid inclusion, the size of the inclusion was observed to increase with progressive excavation, with a cavity of about 1–2 μm appearing at a certain cross-sectional surface (Fig. 3c). The EDS spectra of a smooth part of the exposed surface of the inclusion was obtained, and revealed Na, K, Ca, and Cl as solute elements. Considerable levels of Ga plugged by the ion beam, and Si from the host quartz were also observed (Fig. 3d). O from both ice (H$_2$O) and the host SiO$_2$ were detected. The non-detection of C (0.277 keV) and F (0.677 keV) can be attributed to the negligible abundance of dissolved carbonate species (HCO$_3^-$) and fluorine. However, there is the possibility either 1) that C in HCO$_3^-$ is below the detection limit of the EDS analysis (generally considered to be about 0.1 mass%, which is equivalent to 0.7 mass% of dissolved NaHCO$_3$), or 2) that a small C peak might have been hidden due to absorbance by the host quartz. The present analytical geometry set obstacle host phase in the X-ray path because of the inclined excavated wall (Fig. 3a). This geometric problem precludes quantitative analysis. However, the EDS result shows a considerable amount K which is hardly recognized from the microthermometry experiment and under assumption of simple chemical system (Fig. 3d).

DISCUSSION AND IMPLICATIONS

Although there are few previous reports on metamorphic fluid containing NaCl-KCl-CaCl$_2$, either Ca or K in addition to Na has been observed in several metamorphic terranes. High-salinity CaCl$_2$-bearing brine has been found in some high-P metamorphic rocks in eastern Asia, UHP metamorphic rocks in the Dabie Shan and Sulu region (Rolfo and Ferrando, 2004; Zhang *et al.*, 2005), and HP eclogite in the Dabie Shan (Fu *et al.*, 2002). Rolfo and Ferrando (2004) reported CaCl$_2$-rich (15 mass% CaCl$_2$–2.5mass% NaCl) aqueous fluid as the primary fluid inclusion in OH-rich topaz in UHP quartzite. The aqueous fluid exhibited an isochore crossing at 2.8 GPa and 800°C, and there were indication of the existence of high-density brines under the conditions of the quartz-coesite transition. These observations indicate that the presence of a high-density and high-saline fluid is a possible characteristic of HP-to-UHP metamorphic conditions. Conversely, reports of KCl-bearing fluid inclusions in metamorphic rocks are rare; some have nevertheless being observed as KCl crystals in crustal rocks (e.g., Markl and Bucher, 1998; Okudaira *et al.*, 2017). As far as the use of microthermometry and phase diagrams is concerned, it is difficult to determine the chemical compositions of multi component (>3) aqueous solutions precisely (e.g. Spencer *et al.*, 1990). However, the present observation of NaCl-KCl-CaCl$_2$-bearing fluid inclusions qualitatively indicates the common existence of a KCl component in the metamorphic fluids.

The investigated CaCl$_2$-bearing fluid inclusions were found as intracrystalline fluid inclusion trails in the less-deformed part of the quartz pressure shadows of the investigated Tlc-Grt-Cld schist. This indicates that the fluid inclusions were trapped during the formation stage of the pressure shadows. If the fluids were to have an external origin, perhaps from the fluid infiltration during the exhumation of the rocks, their high salinity would affect the hydrous minerals in the matrix. However, such hydration and increased Cl content of the matrix hydrous minerals were not observed in the investigated sample. This suggests that the observed NaCl-KCl-CaCl$_2$-bearing fluid may have an *in situ* origin. During the formation stage of the quartz pressure shadows, CaCl$_2$-bearing fluids may have been generated from the dehydration reaction that occurred in the garnet. One possible reactant of the dehydration reaction is lawsonite, which is one of the most important water carriers in a cold subduction system (e.g., Pawley, 1994; Kuwatani *et al.*, 2011; Vitale Brovarone *et al.*, 2011; Sato *et al.*, 2016). Orozbaev *et al.* (2015) found polymineralic aggregates mainly composed of clinozoisite, kyanite, and quartz, which had been produced by the decomposition of lawsonite during the exhumation stage. They distinguished the polycrystalline pseudomorphs of lawsonite based on the following observations: (1) the reconstructed composition of the aggregates determined from the modal amounts of clinozoisite, kyanite, and quartz was the same as that of

lawsonite; (2) the cracks that propagated from the poly-phase mineral aggregates were filled with chlorite, indicating that they had been generated by a dehydrated fluid and its hydration reaction with the host garnet; (3) the exhumation *P-T* path of the investigated rock passed the breakdown reaction of lawsonite at around 550°C and 2 GPa. According to the observation of Orozbaev *et al.* (2015), dehydrated fluid might have been released from within the garnet porphyroblasts through cracks and subsequently trapped by the surrounding quartz pressure shadows.

Based on an experimental investigation at about 700°C and 3 GPa, Martin *et al.* (2011) indicated that lawsonite dissolved incongruently into water, with the dissolution product supposed to contain $CaSiO_3(aq) > SiO_2(aq) > Al_2O_3(aq)$, with respect to the mass ratio concentration in the solution. Raman observation did not reveal a detectable amount of water-dissolved SiO_2 or Al_2O_3, and the EDS results also indicated the absence of Al_2O_3 in the fluid inclusion. As Orozbaev *et al.* (2015) reported that the polyphase mineral aggregates containing kyanite crystals, SiO_2 and Al_2O_3 might have not dissolved into water, and could have remained in the solid phase. However, the Ca component might have dissolved into dehydrated water at a considerable degree and exited the host garnet. This solubility contrast may explain the generation processes of the Ca component.

Halter *et al.* (1998) performed a model calculation of the acidic fluid composition (pH 3) equilibrated with a leucogranite at 450°C and 0.4 GPa, with the result suggesting that the aqueous fluid in equilibrium with muscovite contained up to approximately 3 mass% KCl. Although the *P-T* conditions and corresponding whole-rock compositions were different from those of the present study, the experimental and model-based results indicate that dehydration reactions and water-rock interaction under the *P-T* conditions of the investigated sample is capable of generating the observed salt-containing aqueous fluids. Furthermore, the high salinity of the aqueous fluids can be partly explained by the chlorite-forming reaction that occurs on the crack walls, because Na, K, and Ca components do not incorporate into chlorite. During the retrograde metamorphism of crustal constituent rocks, salt-containing aqueous fluids may consume their water component through hydration reactions (i.e., desiccation process) and the precipitated salts are sometimes detectable in the metamorphic rocks (Markl and Bucher, 1998). In the present case, however, the concentrated aqueous fluids may have survived as brine due to the low rate of the hydration reaction.

Aqueous fluids in subduction zones are important because of their effects on geochemical and geophysical processes. At elevated temperatures and pressures, such fluids are capable of dissolving considerable amounts of silicate components (they are referred to as supercritical fluids; e.g., Hermann *et al.*, 2006; Kawamoto *et al.*, 2012), although the dehydration conditions of the lawsonite in the investigated Tlc-Grt-Cld schist are lower temperature than those indicated in these cited previous works. Under such moderate temperature conditions, the dissolved salts in the aqueous fluids act as electrolytes and are also capable of dissolving metal complexes.

CONCLUSION

Previous studies on fluid inclusions in ore deposits and granitic rocks have commonly observed complex chemical systems of the trapped fluids (e.g., Assadzadeh *et al.*, 2016). However, fluid inclusions in metamorphic rocks are assumed to have a rather simple composition. This is because of the difficulty of conducting a detailed analysis, mainly owing to their small sizes and populations.

We conducted conventional fluid inclusion petrography on a Tlc-Grt-Cld schist collected from the Makbal metamorphic complex in Kyrgyz. In addition to textual observation under an optical microscope, Raman analysis, and microthermometry, we attempted cryo-FIB-SEM-EDS analysis of the inclusions to determine the solute species. Although the present observations are only qualitative, they indicate that even fluid inclusions trapped under moderate temperature conditions may contain complex chemical systems that are hardly detectable by microthermometry and other conventional analytical techniques. Misidentification of the solute species introduces errors into salinity estimates, and this may cause propagated inaccuracy in quantitative analytical methods such as LA-ICP-MS. A detailed fluid inclusion petrography would require an accurate quantitative analysis that combines FIB-based sample preparation and cryo-SEM-EDS quantitative analysis. Although this would pose several new questions, they are worth pursuing in a future study.

REFERENCES

Assadzadeh, G. E., Samson, I. M. and Gagnon, J. E. (2016) Identification of fluid inclusion solid phases using a focused ion beam scanning electron microscope with energy dis-

persive spectroscopy: implications for interpreting microthermometric data and composition of fluids in Sn(-W-Mo) deposits. *Can. Mineral.* **54**, 737–754.

Ayora, C. and Fontarnau, R. (1990) X-ray microanalysis of frozen fluid inclusions. *Chem. Geol.* **89**, 135–148.

Bakirov, A. (1978) *Tectonic Position of the Tien-Shan Metamorphic Complexes*. Ilim, Frunze.

Bakirov, A. B., Tagiri, M. and Sakiev, K. S. (1998) Rocks of ultrahigh-pressure metamorphic facies in the Tien Shan. *Russian Geol. Geophys.* **39**, 1709–1721.

Bakker, R. J. (2003) Package FLUIDS 1. Computer programs for analysis of fluid inclusion data and for modelling bulk fluid properties. *Chem. Geol.*, **194**, 3–23.

Baumgartner, M. and Bakker, R. J. (2010) Raman spectra of ice and salt hydrates in synthetic fluid inclusions. *Chem. Geol.* **275**, 58–66.

Bodnar, R. J. (1993) Revised equation and table for determining the freezing point depression of H_2O-NaCl solutions. *Geochim. Cosmochim. Acta* **57**, 683–684.

Desbois, G., Urai, J. L., Burkhardt, C., Drury, M. R., Hayles, M. and Humbel, B. (2008) Cryogenic vitrification and 3D serial sectioning using high resolution cryo-FIB SEM technology for brine-filled grain boundaries in halite: first results. *Geofluids* **8**, 60–72.

Desbois, G., Urai, J. L., Kukla, P. A., Wollenberg, U., Pérez-Willard, F., Radí, Z. and Riholm, S. (2012) Distribution of brine in grain boundaries during static recrystallization in wet, synthetic halite: insight from broad ion beam sectioning and SEM observation at cryogenic temperature. *Contrib. Mineral. Petrol.* **163**, 19–31.

Fu, B., Zheng, Y.-F. and Touret, J. L. R. (2002) Petrological, isotopic and fluid inclusion studies of eclogites from Sujiahe, NW Dabie Shan (China). *Chem. Geol.* **187**, 107–128.

Gao, J. and Klemd, R. (2001) Primary fluids entrapped at blueschist to eclogite transition: evidence from the Tianshan meta-subduction complex in northwestern China. *Contrib. Mineral. Petrol.* **142**, 1–14.

Halter, W. E., Williams-Jones, A. E. and Kontak, D. J. (1998) Modeling fluid-rock interaction during greisenization at the East Kemptville tin deposit: implications for mineralization. *Chem. Geol.* **150**, 1–17.

Heinrich, C. A., Pettke, T., Halter, W. E., Aigner-Torres, M., Audétat, A., Günther, D., Hattendorf, B., Bleiner, D., Guillong, M. and Horn, I. (2003) Quantitative multi-element analysis of minerals, fluid and melt inclusions by laser-ablation inductively-coupled-plasma mass-spectrometry. *Geochim. Cosmochim. Acta* **67**, 3473–3496.

Hermann, J., Spandler, C., Hack, A. and Korsakov, A. (2006) Aqueous fluids and hydrous melts in high-pressure and ultra-high pressure rocks: Implications for element transfer in subduction zones. *Lithos* **92**, 399–417.

Kawamoto, T., Kanzaki, M., Mibe, K., Matsukage, K. N. and Ono, S. (2012) Separation of supercritical slab-fluids to form aqueous fluid and melt components in subduction zone magmatism. *Proc. Nat. Acad. Sci. USA* **109**, 18695–18700.

Konopelko, D., Kullerud, K., Apayarov, F., Sakiev, K., Baruleva, O., Ravna, E. and Lepekhina, E. (2012) SHRIMP zircon chronology of HP-UHP rocks of the Makbal metamorphic

complex in the Northern Tien Shan, Kyrgyzstan. *Gondwana Res.* **22**, 300–309.

Kuwatani, T., Okamoto, A. and Toriumi, M. (2011) Thermodynamic forward modeling of progressive dehydration reactions during subduction of oceanic crust under greenschist facies conditions. *Earth Planet. Sci. Lett.* **307**, 9–18.

Liu, Y., King, H. E., van Huis, M. A., Drury, M. R. and Plümper, O. (2016) Nano-tomography of porous geological materials using focused ion beam-scanning electron microscopy. *Minerals* **6**, 104, doi:10.3390/min604014.

Markl, G. and Bucher, K. (1998) Composition of fluids in the lower crust inferred from metamorphic salt in lower crustal rocks. *Nature* **391**, 781–783.

Martin, L. A. J., Wood, B. J., Turner, S. and Rushmer, T. (2011) Experimental measurements of trace element partitioning between lawsonite, zoisite, and fluid and their implication for the composition of arc magmas. *J. Petrol.* **52**, 1049–1075.

Meyer, M., Klemd, R., Hegner, E. and Konopelko, D. (2014) Subduction and exhumation mechanism of ultra-high and high-pressure oceanic and continental crust at Makbal (Tianshan, Kazakhstan and Kyrgyzstan). *J. Metamorph. Geol.* **32**, 861–884.

Newton, R. C. and Manning, C. E. (2010) Role of saline fluids in deep-crustal and upper-mantle metasomatism: insights from experimental studies. *Geofluids* **10**, 58-72.

Okudaira, T., Shigematsu, N., Harigane, Y. and Yoshida, K. (2017) Grain size reduction due to fracturing and subsequent grain-size-sensitive creep in a lower crustal shear zone in the presence of a CO_2-bearing fluid. *J. Structur. Geol.* **95**, 171–187.

Orozbaev, R., Hirajima, T., Bakirov, A., Takasu, A., Maki, K., Yoshida, K., Sakiev, K., Bakirov, A., Hirata, T., Tagiri, M. and Togonbaeva, A. (2015) Trace element characteristics of clinozoisite pseudomorphs after lawsonite in talc-garnet-chloritoid schists from the Makbal UHP Complex, northern Kyrgyz Tian-Shan. *Lithos* **226**, 98–115.

Pawley, A. R. (1994) The pressure and temperature stability limits of lawsonite: implications for H_2O recycling in subduction zones. *Contrib. Mineral. Petrol.* **118**, 99–108.

Raimburg, H., Thiéry, R., Vacelet, M., Ramboz, C., Cluzel, N., Le Trong, E., Yamaguchi, A. and Kimura, G. (2014) A new method of reconstituting the *P-T* conditions of fluid circulation in an accretionary prism (Shimanto, Japan) from microthermometry of methane-bearing aqueous inclusions. *Geochim. Cosmochim. Acta* **125**, 96–109.

Reyntjens, S. and Puers, R. (2001) A review of focused ion beam applications in microsystem technology. *J. Micromechanic. Microengineer.* **11**, 287–300.

Rolfo, F. and Ferrando, S. (2004) Selected case studies in the high and ultrahigh pressure terranes of Dabie Shan and Sulu (China). *Periodico di Mineralogia* **73**, 173–183.

Samson, I. M. and Walker, R. T. (2000) Cryogenic Raman spectroscopic studies in the system NaCl-$CaCl_2$-H_2O and implications for low-temperature phase behavior in aqueous fluid inclusions. *Can. Mineral.* **38**, 35–43.

Sato, E., Hirajima, T., Yoshida, K., Kamimura, K. and Fujimoto, Y. (2016) Phase relations of lawsonite-blueschists and their role as a water-budget monitor: a case study from the

Hakoishi sub-unit of the Kurosegawa belt, SW Japan. *Eur. J. Mineral*. **28**, 1029–1046.

Scambelluri, M. and Philippot, P. (2001) Deep fluids in subduction zones. *Lithos* **55**, 213–227.

Spencer, R. J., Møller, N. and Weare, J. H. (1990) The prediction of mineral solubilities in natural waters: A chemical equilibrium model for the Na-K-Ca-Mg-Cl-SO$_4$-H$_2$O system at temperatures below 25°C. *Geochim. Cosmochim. Acta* **54**, 575–590.

Tagiri, M., Takiguchi, S., Ishida, C., Noguchi, T., Kimura, M., Bakirov, A. B., Sakiev, K., Takahashi, M., Takasu, A., Bakirov, A. A., Togonbaeva, A. and Suzuki, A. (2010) Intrusion of UHP metamorphic rocks into the upper crust of Kyrgyzian Tien-Shan: *P-T* path and metamorphic age of the Makbal Complex. *J. Mineral. Petrol. Sci.* **105**, 233–250.

Togonbaeva, A., Takasu, A., Bakirov, A. A., Sakurai, T., Tagiri, M., Bakirov, A. B. and Sakiev, K. (2009) CHIME monazite ages of garnet-chloritoid-talc schists in the Makbal Complex, Northern Kyrgyz Tien-Shan: First report of the age of the UHP metamorphism. *J. Mineral. Petrol. Sci.* **104**, 77–81.

Togonbaeva, A., Takasu, A., Tagiri, M., Bakirov, A. B., Bakirov, A. A. and Sakiev, K. (2010) Newly described eclogites from the Neldy Formation, Makbal district, Northern Tien-Shan, Kyrgyzstan. *J. Mineral. Petrol. Sci.* **105**, 80–85.

Tsujimori, T., Sisson, V., Liou, J., Harlow, G. and Sorensen, S. (2006) Very-low-temperature record of the subduction process: A review of worldwide lawsonite eclogites. *Lithos* **92**, 609–624.

Vitale Brovarone, A., Groppo, C., Hetenyi, G., Compagnoni, R. and Malavieille, J. (2011) Coexistence of lawsonite-bearing eclogite and blueschist: phase equilibria modelling of Alpine Corsica metabasalts and petrological evolution of subduction slabs. *J. Metamorph. Geol.* **29**, 583–600.

Whitney, D. L. and Evans, B. W. (2010) Abbreviations for names of rock-forming minerals. *Amer. Mineral.* **95**, 185–187.

Wirth, R. (2004) Focused Ion Beam (FIB) A novel technology for advanced application of micro-and nanoanalysis in geosciences and applied mineralogy. *Eur. J. Mineral.* **16**, 863–876.

Yoshida, K., Hirajima, T., Ohsawa, S., Kobayashi, T., Mishima, T., and Sengen, Y. (2015) Geochemical features and relative B-Li-Cl compositions of deep-origin fluids trapped in high-pressure metamorphic rocks. *Lithos* **226**, 50–64.

Yoshida, K., Hirajima, T., Miyake, A., Tsuchiyama, A., Ohi, S., Nakano, T. and Uesugi, K. (2016) Combined FIB microsampling and X-ray microtomography: a powerful tool for the study of tiny fluid inclusions. *Eur. J. Mineral.* **28**, 245–256.

Zhang, Z., Shen, K., Xiao, Y., Van Den Kerkhof, A. M., Hoefs, J. and Liou, J. G. (2005) Fluid composition and evolution attending UHP metamorphism: study of fluid inclusions from drill cores, southern Sulu Belt, Eastern China. *Int. Geol. Rev.* **47**, 297–309.